Published in final edited form as:
J Neurochem. 2009 January ; 108(2): 450–464. doi:10.1111/j.1471-4159.2008.05781.x.

Brain-Derived Neurotrophic Factor in Arterial Baroreceptor Pathways: Implications for Activity-Dependent Plasticity at Baroafferent Synapses

Jessica L. Martin[1,2], **Victoria K. Jenkins**[1], **Hui-ya Hsieh**[1], and **Agnieszka Balkowiec**[1,2,3]

1 *Department of Integrative Biosciences, Oregon Health and Science University, Portland, OR*

2 *Neuroscience Graduate Program, Oregon Health and Science University, Portland, OR*

3 *Department of Physiology and Pharmacology, Oregon Health and Science University, Portland, OR*

Abstract

Functional characteristics of the arterial baroreceptor reflex change throughout ontogenesis, including perinatal adjustments of the reflex gain and adult resetting during hypertension. However, the cellular mechanisms that underlie these functional changes are not completely understood. Here, we provide evidence that brain-derived neurotrophic factor (BDNF), a neurotrophin with a well-established role in activity-dependent neuronal plasticity, is abundantly expressed *in vivo* by a large subset of developing and adult rat baroreceptor afferents. Immunoreactivity to BDNF is present in the cell bodies of baroafferent neurons in the nodose ganglion (NG), their central projections in the solitary tract, and terminal-like structures in the lower brainstem *nucleus tractus solitarius* (NTS). Using ELISA *in situ* combined with electrical field stimulation, we show that native BDNF is released from cultured newborn NG neurons in response to patterns that mimic the *in vivo* activity of baroreceptor afferents. In particular, high-frequency bursting patterns of baroreceptor firing, which are known to evoke plastic changes at baroreceptor synapses, are significantly more effective at releasing BDNF than tonic patterns of the same average frequency. Together, our study indicates that BDNF expressed by first-order baroreceptor neurons is a likely mediator of both developmental and post-developmental modifications at first-order synapses in arterial baroreceptor pathways.

Keywords

Calcium channels; Electrical field stimulation; Frequency-dependent depression; Nodose ganglion; Nucleus tractus solitarius

INTRODUCTION

The arterial baroreceptor reflex plays a crucial role in cardiovascular homeostasis by controlling arterial blood pressure (Brooks and Sved 2005; Guyenet 2006). The afferent limb of the reflex includes mechanosensitive neurons with cell bodies in the nodose-petrosal ganglion complex (NPG), peripheral endings in the cardiac outflow tract, such as the aortic arch, and central projections terminating in the medial *nucleus tractus solitarius* (NTS) of the dorsal medulla (Andresen and Kunze 1994; Guyenet 2006). The natural stimulus for these neurons is a distention of the arterial wall by an increase in blood pressure (Guyenet 2006).

Correspondence should be addressed to Dr. Agnieszka Balkowiec, Department of Integrative Biosciences, Oregon Health and Science University School of Dentistry, 611 S.W. Campus Drive, Portland, OR 97239; Tel: (503) 418-0190; Fax: (503) 494-8554; E-mail: balkowie@ohsu.edu.

Arterial baroreceptors are active in the fetus, but the functional characteristics of the baroreceptor reflex undergo significant changes during the perinatal period (Segar 1997). For example, the gain of the reflex increases several-fold between the first and second week of age in mice (Ishii *et al.* 2001). In fact, the reflex remains plastic throughout adulthood, as is manifested by its ability to reset the operating range of blood pressures while maintaining unchanged reflex sensitivity (Kunze 1981; Heesch *et al.* 1984a; Heesch *et al.* 1984b; Kunze 1986; Andresen and Yang 1989; Xie *et al.* 1991). In addition, increasing frequency of baroreceptor input leads to frequency-dependent depression of the postsynaptic responses in the NTS neurons (Scheuer *et al.* 1996; Chen *et al.* 1999; Liu *et al.* 1998; Liu *et al.* 2000; Doyle and Andresen 2001), a form of synaptic plasticity that may influence baroreflex function (Liu *et al.* 2000). However, the exact molecular mechanisms underlying changes in either the perinatal or adult system are not well understood.

In recent years, brain-derived neurotrophic factor (BDNF), a member of the neurotrophin family of growth factors, has emerged as a key mediator of mechanisms regulating activity-dependent synaptic maturation and plasticity (Huang and Reichardt 2001; Poo 2001), including sensory plasticity (Malcangio and Lessmann 2003). During embryonic development, BDNF is required for the survival of a large subset of NPG neurons, including cardio-respiratory control neurons (Erickson *et al.* 1996), and specifically arterial baroreceptors (Brady *et al.* 1999). Namely, BDNF is expressed in the fetal cardiac outflow tract, and acts as a target-derived survival factor for developing baroreceptor afferents (Brady *et al.* 1999). After birth, when NPG neurons no longer depend on BDNF for survival (Brady *et al.* 1999), BDNF is expressed by a significant proportion of NPG neurons (Schecterson and Bothwell 1992; Wetmore and Olson 1995; Apfel *et al.* 1996; Zhou *et al.* 1998) and released from these neurons by activity (Balkowiec and Katz 2000). There is also evidence suggesting that BDNF is a modulator of visceral sensory transmission (Balkowiec *et al.* 2000), raising the possibility that BDNF is involved in maturation and/or plasticity in the arterial baroreceptor pathway.

The present study was undertaken to test the following hypotheses: 1) BDNF is present in baroreceptor afferents *in vivo*, and 2) BDNF release from cultured nodose ganglion (NG) neurons is regulated by stimulation patterns that mimic *in vivo* activity of baroreceptor afferents.

MATERIALS AND METHODS

Animals

Postnatal day (P) 0–2, P9, P23 and P30 Sprague Dawley rats (Charles River Laboratories, Wilmington, MA) were used for this study. All procedures were approved by the Institutional Animal Care and Use Committee of the Oregon Health and Science University, and conformed to the *Policies on the Use of Animals and Humans in Neuroscience Research* approved by the Society for Neuroscience.

DiI-labeling of baroreceptor afferents

P2 rats were deeply anesthetized by hypothermia, and either right or both aortic depressor nerves (ADN) exposed in the neck by a ventral midline incision, and isolated from surrounding tissues with Parafilm “M” (Pechiney Plastic Packaging, Menasha, WI). The fluorescent lipophilic dye CM-DiI (Cell Tracker® urotrace® issue-labeling paste; Invitrogen, Carlsbad, CA) was placed on the uncut nerve, and the region isolated with a fast hardening silicone elastomer (Kwik-Sil; WPI), as previously described (Balkowiec *et al.* 2000). The animals were then sutured and allowed to recover for either 7, 21 or 28 days. Following the perfusion and before the tissue collection, the position of the dye was verified, and the animals with evidence of dye displacement were excluded from the study.

Preparation of nodose ganglia (NG), brainstems and NG cultures for immunostaining

Rats were euthanized and perfused transcardially with phosphate-buffered saline (PBS), followed by 2% paraformaldehyde in 0.1 M sodium phosphate buffer, in some experiments supplemented with 0.2% parabenzoquinone. NGs and brainstems were dissected and post-fixed with the fixative of the same composition as the one used in perfusion, for 30 min (NGs) or 2 h (brainstems), followed by rinsing in PBS and cryoprotection in 30% sucrose in PBS at 4ºC for at least 24 h. Next, NGs and brainstems were embedded in O.C.T. Tissue-Tek® ompound (Sakura Finetek USA, Inc., Torrance, CA) and blocks of tissue were sectioned on a cryostat at 10 μ (NGs) or 30 μm (brainstems). NG sections were collected onto glass slides, whereas brainstem sections were collected into PBS to be processed as free-floating sections. Following tissue cutting, NG and brainstem sections were screened for the presence of DiI in NG somata and the brainstem NTS. Sections were discarded if no DiI was present in the NG or brainstem. Furthermore, sections were discarded if there was evidence of DiI spread beyond the ADN, e.g. DiI fluorescence in a majority of the NG somata, or in neuronal cell bodies in the brainstem dorsal motor nucleus of vagus, or nucleus ambiguus. Our overall success rate with the DiI labeling of ADN afferents was approximately 18% (15 of 81 labeled animals across all three time points). Both NG and brainstem sections were collected in a series of two and every other section (i.e. one series) was processed for BDNF immunostaining. For double immunofluorescence in NGs, both series were processed: one for BDNF and HCN1 and the other for BDNF and TRPV1 (VR1, N-terminus), resulting in alternate sections being stained for each marker, i.e. HCN1 and TRPV1. NG cultures for immunostaining were fixed with 2% paraformaldehyde and 0.2% parabenzoquinone in 0.1 M sodium phosphate buffer, pH 7.4, for 30 min at room temperature.

Immunostaining of sections

Sections were (1) incubated for 1 h in a 10% solution of goat serum in dilution buffer (DB; 0.02 M phosphate buffer, 0.5 M NaCl, 0.3% Triton X-100), (2) incubated for 2 h in chicken polyclonal anti-BDNF [1:50 (NGs) or 1:25 (brainstems); Promega, Madison, WI] in DB, applied alone, or in combination with either rabbit polyclonal anti-HCN1 (1:100; Alomone Labs, Jerusalem, Israel) or rabbit polyclonal anti-VR1 (TRPV1), N-terminus (1:500; Neuromics, Edina, MN), (3) washed three times in DB, (4) incubated in secondary antibody diluted in DB with 10% goat serum as specified for the following types of immunostaining: (i) *NG, immunodetection of BDNF only*, 1 h in goat anti-chicken biotinylated IgG (1:200, Vector Laboratories, Burlingame, CA), (ii) *brainstem, immunodetection of BDNF only*, 2 h in donkey anti-chicken IgG-Cy2 (1:200, Jackson Immunoresearch; West Grove, PA), (iii) *NG, double immunodetection of either BDNF/HCN1 or BDNF/VR1 (TRPV1)*, 1 h in goat anti-chicken IgG-Alexa 488 (1:1000, Invitrogen, Carlsbad, CA) and goat anti-rabbit IgG-Alexa 647 (1:1000, Invitrogen, Carlsbad, CA), (5) washed three times in PBS, (6) incubated for 30 min in avidin-biotin reagent (ABC) in PBS-0.5M NaCl (1:100, Vectastain *Elite*, Vector Laboratories;), (7) washed for 10 min in PBS-0.5M PBS, (8) washed two times in PBS, (9) incubated for 3–5 min in diaminobenzidine (DAB) solution (in PBS: 0.3 mg/ml DAB, 0.032% $NiCl_2$, 0.0075% H_2O_2), (10) washed three times in PBS, and (11) mounted with Gel Mount (Sigma) or FluorSave (Calbiochem, San Diego, CA). For the fluorescent method (brainstem and double-immunostaining in NG), steps 6–10 were omitted.

Double-immunostaining of cultures for BDNF and Neurofilament, a pan-neuronal marker

Cultures were (1) incubated for 1 h in 1:1 solution of goat serum and PBS-0.1% Triton X-100, (2) incubated for 2 h in chicken polyclonal anti-BDNF (1:100; Promega) alone or combined with mouse monoclonal anti-neurofilament 68 and 160 (1:100; Sigma, St. Louis, MO), diluted in PBS-0.1% Triton X-100 with 10% goat serum, (3) washed one time in PBS followed by two washes in PBS containing 5% goat serum, (4) incubated for 1 h in goat anti-chicken biotinylated

IgG (1:200, Vector Laboratories) alone or combined with goat anti-mouse IgG-Cy3 (1:200, Jackson Immunoresearch), diluted in PBS-0.1% Triton X-100 with 10% goat serum, (5) washed in PBS, (6) incubated for 30 min in avidin-biotin reagent in PBS-0.5M NaCl (1:100, Vectastain *Elite*, Vector Laboratories), (7) incubated for 10 min in PBS-0.5M PBS, (8) washed two times in PBS, (9) incubated for 3–5 min in DAB solution, (10) washed once in PBS, and (11) mounted with ProLong® Gold (Invitrogen) or Gel Mount (Sigma).

For immunostaining in both sections and cultures, to minimize a non-specific staining, the anti-BDNF antibody was precleared by overnight incubation with vibratome slices (40 μm) of a 2% or 4% paraformaldehyde-fixed adult rat cerebellum (approximately 1/3 of cerebellum per 1 ml of the antibody solution). All staining procedures were performed at room temperature.

Testing specificity of the BDNF antibody

Western blotting—Recombinant human BDNF (Promega) was diluted in loading buffer (130 mM Tris-Cl, 20% glycerol, 4.6% SDS, 5% β-mercaptoethanol, 0.2% bromophenol blue) to yield 2000 ng, 200 ng, and 40 ng samples. Proteins and ladder (SeeBlue Plus2, Invitrogen, Carlsbad, CA) were resolved on a 12% (w/v) SDS-PAGE gel, and electrotransferred to a PVDF membrane. Membranes were incubated in blocking solution (150 mM NaCl, 50 mM Tris-Cl, pH 7.4, with 5% dry milk) for 30 min, then incubated with chicken polyclonal anti-BDNF (1:50 in blocking solution) overnight at 4°C. Following three Tris-buffered saline (TBS, 150 mM NaCl, 50 mM Tris-Cl, pH 7.4) washes, the membranes were incubated with the rabbit anti-chicken IgY-horseradish peroxidase (HRP; 1:1000 in blocking solution, Promega) for 1 hour at 25°C, and washed 3 times in TBS. HRP was activated with chemiluminescent reagents (Western Lightning, Perkin-Elmer, Waltham, MA) for 90 sec, and blue X-ray film (Phenix Research, Candler, NC) was exposed for 2 min.

Preabsorption with BDNF protein—Chicken polyclonal anti-BDNF (Promega, Madison, WI) was preabsorbed by incubation with BDNF-coated beads. Magnetic beads with surface tosyl groups (Dynabead M-280 Tosylactivated, Invitrogen) were coated with BDNF protein (1.25 μg BDNF, R&D Systems, Minneapolis, MN, per 2×10^7 beads) according to the manufacturer's instructions, with the exception of using a sodium-phosphate/borate buffer (0.075 M NaH_2PO_4, 0.075 M Na_2HPO_4, 0.1 M H_3BO_4, pH 9.5) during the coating step.

After incubation with beads, no detectable BDNF remained in the solution (unbound to beads), as determined by a sandwich ELISA (BDNF E_{max}™ ImmunoAssay System; Promega), and the estimated density of BDNF bound to beads was approximately 2.4 fg/μm^2. Moreover, after incubation with chicken polyclonal anti-BDNF (see below), BDNF-coated beads exhibited five-fold greater immunoreactivity (measured as the optical density of the reaction product; BDNF E_{max}™ ImmunoAssay System; Promega) than uncoated beads.

Chicken polyclonal anti-BDNF was diluted (1:50) in PBS-powdered bovine serum albumin (BSA, 0.1% w/v, pH 7.4) and precleared with cerebellar slices, as described above for staining cultures. BDNF-coated and uncoated beads were then incubated with the precleared anti-BDNF for 1h at room temperature with rotation. Next, beads were pelleted with a magnet, and the supernatant (containing only the unbound fraction of the antibody) was collected and immediately used to stain NG cultures, as described above.

Specificity of other antibodies used—NG and brainstem sections, and NG cultures were stained according to the methods described above, except that primary antibodies were omitted. Under these conditions, the specimens were devoid of staining for all secondary antibodies used (data not shown). Specificity of other primary antibodies used in this study has been previously demonstrated (anti-HCN1, Doan et al., 2004; anti-TRPV1, Bennett *et al.*, 2003).

Microscopy, digital imaging, and image analysis

All NG cultures and sections were imaged with an Olympus IX-71 inverted microscope (Olympus America Inc., Center Valley, PA), and images were captured with a Hamamatsu ORCA-ER CCD camera (Hamamatsu, Bridgewater, NJ) controlled by either Wasabi (Hamamatsu) or Olympus Microsuite software (vs. 5.0, Olympus America Inc). In addition, BDNF expression in DiI-labeled baroreceptor terminals in the brainstem was examined using a BioRad Radiance 2100 confocal microscope (BioRad, Hercules, CA). Confocal images of the two fluorophores, DiI and Cy2, were taken sequentially with a 63x oil-immersion objective with an additional 3x confocal zoom factor as a series of z-stacks of 0.5–0.75 μm thickness. All images were taken from the medial NTS ipsilateral to the DiI placement. Images were analyzed and adjusted for brightness and contrast using ImageJ software (National Institutes of Health, Bethesda, MD).

In order to determine the degree of DiI and BDNF colocalization in the NG somata, all DiI-labeled profiles containing a nucleus from every other section of the NG were selected blinded to BDNF content. Subsequently, the images were overlaid and BDNF content was assessed. BDNF-IR somata exhibited a characteristic perinuclear punctate ring. In a subset of P30 animals, BDNF staining was combined with immunostaining for HCN1 or VR1 (TRPV1, N-terminus). Similar to analysis of BDNF IR alone, DiI-positive NG somata containing a nucleus were analyzed for the presence of BDNF and either HCN1 or VR1.

In order to determine DiI and BDNF colocalization in the brainstem puncta, 25 DiI-labeled puncta were selected throughout the rostro-caudal extent of the medial NTS, ipsilateral to the DiI-labeled ADN, randomly selected, blind to the BDNF content. Images containing DiI and BDNF IR were overlaid, and BDNF IR was assessed.

The cross-sectional area of DiI-labeled P30, unlabeled P0, and unlabeled P30 NG cell bodies was measured in sections single-stained for BDNF (the ABC method) using ImageJ software. Specifically, the cell perimeter was outlined and enclosed area was computed and recorded. In addition to DiI-labeled cells, the entire NG neuron population was sampled, and BDNF content, along with the cross-sectional area, were assessed in the right side P0 and P30 ganglia from three rats each. Every 10^{th} NG section (approximately 100 μm apart from each other) was digitally imaged, and each cell that contained a nucleus was assessed for its BDNF content and the cross-sectional area. For each age, all data from the three rats were subsequently pooled and plotted as frequency histograms of cross-sectional areas. The cell size distribution was compared between BDNF-IR and BDNF-non-IR cells in the sample of the entire NG population.

Preparation of NG cultures

P0-P1 (3–48 h old) and P9 rat pups were euthanized by intraperitoneal injection of Euthasol (0.1 mg/kg) and decapitated. NGs were rapidly and aseptically dissected from each animal in ice-cold Ca^{2+}/Mg^{2+}-free Dulbecco's phosphate-buffered salt solution (Mediatech, Herndon, VA). The ganglia were next digested in 0.1% crystallized trypsin-3X (Worthington Biochemical Corp., Lakewood, NJ), followed by 0.2% collagenase (Sigma), 30 min each, at 37°C in a humidified atmosphere of 5% CO_2 and 95% air. Both enzymes were dissolved in Ca^{2+}/Mg^{2+}-free Hanks' balanced salt solution (Mediatech) which had been pre-incubated for at least 2 h at 37°C in a humidified atmosphere of 5% CO_2 and 95% air. Following the enzymatic treatment, NGs were rinsed twice: first in 0.1% soybean trypsin inhibitor (Worthington) dissolved in Ca^{2+}/Mg^{2+}-containing Dulbecco's phosphate-buffered salt solution (Mediatech), and next in plating medium, both at room temperature. The tissue was next transferred to the plating medium and triturated through fire-polished Pasteur pipettes of decreasing tip diameter. Dissociated NG cells were plated in UV-sterilized, 96-well, flat bottom

ELISA plates (MaxiSorp™, Nalge Nunc Int., Naperville, IL) pre-coated with anti-BDNF capture antibody (BDNF E_{max}™ ImmunoAssay System, Promega; for BDNF ELISA *in situ*; Balkowiec and Katz 2000), and/or in 24-well tissue culture-treated polystyrene plates (Corning Inc., Corning, NY) on poly-D-lysine (0.1 mg/ml; Sigma) and laminin (0.4 μg/ml; Sigma)-coated glass coverslips (for immunocytochemistry). NG cultures were grown in Neurobasal-A plating medium (Invitrogen) supplemented with B-27 serum-free supplement (Invitrogen), 0.5 mM L-glutamine (Invitrogen), 2.5% fetal bovine serum (HyClone, Logan, UT), 1% Penicillin-Streptomycin-Neomycin antibiotic mixture (Invitrogen), and in some experiments, 2.5% Nystatin (Sigma), for 3 days at 37°C in a humidified atmosphere of 5% CO_2 and 95% air.

Electrical field stimulation

Following the initial 3-day incubation, NG cultures were stimulated in 96-well plates as recently described by our laboratory (Buldyrev *et al.* 2006). Specifically, the wells were fitted with paired Ag/AgCl electrodes (0.25 mm wire diameter; one pair per well), connected in parallel (four wells per set) to one of four independent outputs of the stimulator (MultiStim System; Digitimer; Welwyn Garden City, Hertfordshire, UK). The stimulation pattern delivered by each of the outputs was controlled by the 8-channel programmable pulse generator Master-8-cp (AMPI, Jerusalem, Israel). Four additional wells were also fitted with pairs of electrodes, but were not connected to the stimulator and served as controls. The plate was put back to the incubator, and the neurons were stimulated with biphasic rectangular pulses of 0.5 ms duration and amplitude of 80–120 mA per well, delivered at various patterns (see Results).

Drug treatment

Cultures were treated with the drugs for 30 min prior to electrical stimulation, at 37°C in a humidified atmosphere of 95% air/5% CO_2. ω-Conotoxin GVIA (Sigma) was dissolved in distilled water and used at the final concentration of 1 μM, and nimodipine (Sigma) was dissolved in ethanol and used at the final concentration of 2 μM.

Measurement of BDNF release

BDNF protein was measured with a modified sandwich ELISA, termed ELISA *in situ*, as previously described (Balkowiec and Katz 2000). Specifically, 96-well ELISA plates were UV-sterilized for 20 min and coated with anti-BDNF monoclonal capture antibody (BDNF E_{max}™ ImmunoAssay System, Promega) at 4°C for 12–18 h. Next, plates were washed and blocked, followed by two 1-h (or longer) incubations with culture medium to remove any residue of the ELISA washing solution. Then, NG cultures were prepared as described above, plated in anti-BDNF-coated wells, and grown for three days. The BDNF E_{max}™ ImmunoAssay System (Promega) was used according to the protocol of the manufacturer, except that the concentration of the anti-BDNF monoclonal and anti-human BDNF polyclonal antibody was 3 μg/ml and 2 μg/ml, respectively, and the dilution of the anti-IgY-HRP antibody was 1:100. All reagents used prior to cell plating were sterilized with a 0.2 μm syringe filters (Millex® GP, Millipore, Carrigtwohill, Ireland). BDNF samples used to generate standard curves were incubated in the same plate as the NG cell culture. Following cell stimulation and a 1-h post-stimulus incubation, plates were extensively washed to remove all cells and cell debris, and the anti-human BDNF polyclonal antibody was applied, followed by subsequent steps according to the manufacturer's protocol. Absorbance values were read at 450 nm in a plate reader (V_{max}™, Molecular Devices, Sunnyvale, CA).

Calculations and statistical analysis

BDNF localization studies—The percentage of BDNF-IR NG somata or brainstem puncta within the DiI-labeled (putative baroreceptor) population was calculated for each animal. The

mean percentages of BDNF-IR DiI-containing profiles were compared among three time points, i.e. P9, P23 and P30, using a one-way ANOVA, followed by Tukey's posthoc test. Furthermore, an independent sample, two-tailed *t*-test was used to make the following comparisons: (i) the mean percentage of BDNF-IR NG somata in the entire population of NG neurons at P0 *versus* P30, (ii) the mean percentage of BDNF-IR neurons between the entire NG population and the DiI-containing NG at P30, and (iii) the mean percentage of BDNF-IR profiles between DiI-containing somata in the NG and DiI-containing puncta in the medial NTS at P30. Data are expressed as mean ± standard error. $P < 0.05$ was considered significant.

BDNF release studies—BDNF levels were calculated from the standard curve prepared for each plate, using SOFTmax PRO® vs. 4.3 software (Molecular Devices). The standard curves were linear within the range used (0–500 pg/ml) and the quantities of BDNF in experimental samples were always within the linear range of the standard curve. Data are expressed as mean ± standard error. Samples were compared using ANOVA followed by Duncan's multiple comparison procedure, and $P < 0.05$ was considered significant.

RESULTS

Brain-derived neurotrophic factor (BDNF) is abundantly expressed in aortic baroreceptor neurons *in vivo*

A subset of developing visceral sensory neurons from the nodose-petrosal ganglion complex (NPG) expresses BDNF as early as embryonic day 16 (Brady *et al.* 1999). BDNF mRNA and protein have also been detected in a subset of adult NPG neurons (Schecterson and Bothwell 1992; Wetmore and Olson 1995; Apfel *et al.* 1996; Zhou *et al.* 1998; Ichikawa *et al.* 2007). However, the functional identity of the BDNF-expressing population is, for the most part, unknown. Thus far, only the tyrosine hydroxylase-expressing subpopulation of chemoafferent neurons has been identified as containing a portion of the BDNF-positive neurons (Brady *et al.* 1999). Therefore, we tested the hypothesis that BDNF is also found in aortic baroreceptor neurons, whose cell bodies are located in the nodose ganglion (NG), using BDNF immunohistochemistry.

We first conducted several control experiments to verify the specificity of the BDNF antibody. Recombinant human BDNF protein was applied to an SDS-PAGE gel and immunoblotted with the BDNF antibody. The 27-kDa BDNF protein was monomerized by reducing agents in the loading buffer, yielding a monomer of approximately 13 kDa. The 2000 ng and 200 ng samples of BDNF were detected, but not the 40 ng sample, using the Western blot technique (Fig. 1A). Consistent with this result, we were not able to detect BDNF in the NG, in which total levels of BDNF are in the picogram range, as confirmed by ELISA (data not shown). The specificity of the BDNF antibody was further assessed with a modified preabsorption assay. BDNF protein was covalently linked to magnetic beads and then incubated with the BDNF antibody, providing a novel way to separate BDNF-antibody complexes from unbound antibody. The supernatant, potentially containing any antibody that did not bind to the BDNF-coated beads, was used to stain NG cultures. Cultures stained with antibody preabsorbed with BDNF immobilized on beads (Fig. 1B, 'preabsorbed') showed markedly reduced BDNF IR compared to cultures stained with the antibody incubated with uncoated beads (Fig. 1B, 'control'). Furthermore, the pattern of staining in NG sections and the caudal brainstem matches results obtained using different anti-BDNF antibodies (Ichikawa *et al.*, 2007).

The peripheral processes of aortic baroreceptor neurons travel largely unaccompanied (Cheng *et al.* 1997) in the aortic depressor nerve, thus allowing us to isolate aortic baroreceptor neurons for neuronal tracing studies. The right side aortic depressor nerve was pre-labeled at P2 with the fluorescent tracer CM-DiI. Following 7, 21 and 28 days *in vivo*, sections of ipsilateral NGs from P9 (n=6 rats), P23 (n=3 rats) and P30 (n=5 rats), respectively, were processed for BDNF

immunohistochemical staining (Fig. 2A, B). All DiI-labeled somata also containing a nuclear profile were identified in every other section of the ganglion, and BDNF immunoreactivity was assessed for every DiI-labeled profile meeting these criteria.

At P9, an average of 46.3 ± 8.1 DiI-labeled profiles were found, and among these, 26.7 ± 5.1 were BDNF-IR (n = 6 NG). At P23, an average of 35.7 ± 7.8 DiI-labeled profiles were found, and 12.7 ± 4.2 of these cells were BDNF-IR (n = 3 NG). Similarly at P30, an average of 30.2 ± 5.5 DiI-labeled profiles were found, and 12 ± 2.2 of these cells showed BDNF IR (n = 5 NG). The percentage of neuronal somata that contain BDNF IR significantly decreases between P9 and P23 ($P<0.01$) but, subsequently, remains unchanged between P23 and P30, in the DiI-labeled putative baroreceptor population (Fig. 2C). These data indicate that BDNF is expressed by a majority of baroreceptor afferents during early postnatal development, and the number of BDNF-IR baroafferents remains high even after the period of postnatal maturational changes in the baroreceptor reflex.

BDNF immunoreactivity is present in baroreceptor afferents of all sizes

Baroreceptor afferents are divided into two broad categories: larger, myelinated (Aδ) and smaller unmyelinated (C) fibers, each serving a distinct function in the baroreceptor reflex (Chapleau and Abboud 1989; Chapleau *et al.* 1989; Seagard *et al.* 1993). In order to begin addressing the question of whether BDNF is associated with a specific subtype of baroreceptor afferents, we first examined the cell size distribution of BDNF-IR, compared with BDNF-non-IR, DiI-labeled cells from P30 NG. For this analysis, we used the same cell population that was selected for counting percentages of BDNF-IR baroafferents. A total of 60 BDNF-IR and 91 BDNF-non-IR were identified in 5 ganglia, and the cross-sectional area of each cell was determined as described in the 'Materials and Methods' section. Our data indicate that the BDNF-IR subpopulation of baroafferents is not limited to neurons of a specific size range and, instead, spans the entire range of cell sizes found for the DiI-labeled aortic baroreceptors, including the least abundant myelinated A-fibers that are associated with the largest cell bodies. In fact, when comparing among various cell sizes, the proportion of BDNF-IR cells is greater in larger neurons (Figure 3A).

For comparison, we examined the cell size distribution of BDNF-IR and BDNF-non-IR cells in the entire population of P30, as well as P0, NG neurons. Sections of three P30 and three P0 right-side ganglia single-stained for BDNF (ABC method; Fig. 3B, C, insets) were used for the analysis. One-thousand-six-hundred-thirteen neurons from three P30 ganglia were measured, including 1047 BDNF-IR cells. Similar to the cell size distribution of BDNF-IR baroreceptors, BDNF-IR NG afferents, sampled from the whole NG population at P30, are distributed across the entire size range (Fig. 3B). This result indicates that the distribution pattern of BDNF expression among baroreceptor afferents is shared with other subpopulations of NG neurons at this age. We also examined P0 NG neurons and, here too, BDNF IR was present in all cell sizes found in this age group (1675 BDNF-IR cells out of 2540 cells sampled from 3 ganglia; Fig. 3C). In both P0 and P30 ganglia, the proportion of BDNF-IR cells is greater in neurons of larger cross-sectional area. These data suggest that the distribution of BDNF expression among various subpopulations of NG neurons does not change during the postnatal maturational period. In addition, the percentage of BDNF-IR cells in the entire NG neuron population does not significantly change between P0 (66%) and P30 (65%). Moreover, the overall mean percentage of BDNF-IR baroreceptor somata at P30 (40%) is significantly lower compared to the mean percentage of BDNF-IR somata in the entire NG population (65%; $P<0.01$). This indicates that the developmental decline in BDNF expression observed for the baroreceptor population (Fig. 2C) is not a general phenomenon that affects the NG population as a whole.

BDNF immunoreactivity is present in large subsets of HCN1- and TRPV1- expressing baroreceptor afferents

To further explore the functional identity of BDNF-IR baroreceptor afferents, we next turned to histochemical markers selective for specific subpopulations of NG afferents. Doan and colleagues (2004) have found the hyperpolarization-activated cyclic nucleotide-gated ion channel protein 1 (HCN1) to be expressed in myelinated, but not unmyelinated, baroreceptor terminals. Therefore, we first examined BDNF IR in HCN1-IR DiI-labeled NG neurons (putative baroreceptor afferents) from P30 animals. Out of 84 DiI-labeled cells, 18 expressed HCN1 IR, and 8 showed double HCN1/BDNF IR. These data indicate that HCN1-IR cells constitute approximately 21% of the DiI-labeled population, and nearly a half of them show BDNF IR, similar to HCN1-non-IR cells (Fig. 4A, Table 1).

A marker selective for unmyelinated NG afferents is the vanilloid receptor TRPV1 (Jin *et al.*, 2004). Moreover, functional TRPV1 channels are present exclusively in unmyelinated, C-type aortic baroreceptors (Reynolds *et al*., 2006). Therefore, we used TRPV1, combined with BDNF, immunostaining in order to examine BDNF expression in unmyelinated baroafferents. We find that one-half of baroafferents identified by the DiI labeling of the aortic depressor nerve express TRPV1 (28 out of 51 DiI-labeled cells; Table 1). From those cells, almost 60% exhibit BDNF IR (Fig. 4B, Table 1). Within the TRPV1-non-IR baroreceptor population, on the other hand, only one-third contains BDNF IR. Together, these results are consistent with our cell size distribution analysis indicating that BDNF is present in both small unmyelinated, and large myelinated baroafferents.

BDNF immunoreactivity is present in the central projections of baroreceptor afferents in the brainstem

During development, nodose-petrosal ganglion (NPG) neurons are dependent on target-derived BDNF for survival (Erickson *et al*. 1996), but this dependence is lost by the first postnatal day (Brady *et al.* 1999). Consequently, BDNF expressed by postnatal baroreceptor neurons is likely to play other roles, such as promoting maturation and/or modulating the function of baroreceptor synapses in the medial *nucleus tractus solitarius* (NTS) of the lower brainstem. In support of this possibility, BDNF has previously been shown to be anterogradely transported in the central axons of dorsal root ganglion sensory neurons (Zhou and Rush 1996). Therefore, we next asked whether BDNF is present in the central afferent tract as well as the central terminal field of baroreceptor neurons in the NTS. For these studies, we used the same DiI-labeled P30 rats (i.e. 28 days post-labeling) that were used in the studies of BDNF distribution in baroreceptor cell bodies described above. P9 and P23 rats, which represent shorter DiI-transport times (i.e. 7 and 21 days, respectively) were not used in this analysis.

Using confocal microscopy, we examined the distribution of BDNF IR in the central projections of baroreceptor afferents in five P30 brainstems. Specifically, we examined the solitary tract, which contains the central axons of NPG neurons, and the medial NTS, the major central target of baroreceptor afferents (Andresen and Kunze 1994). In all P30 brainstems examined, strong BDNF IR was observed in the solitary tract (Figure 5A, B), suggesting that BDNF is transported to central terminals in visceral afferent neurons. BDNF IR was also present in DiI-labeled synaptic terminal-like puncta in the medial NTS (Fig. 5C, D). The distribution of BDNF in the central projections of baroreceptor afferents closely matched the BDNF distribution in the cell bodies of these neurons for each of the 5 animals examined (Fig. 5E). Moreover, out of a total of 125 DiI-labeled terminal-like puncta identified in the NTS from 5 brainstems, 56 (44.8%) were also BDNF-IR. This percentage closely matches the percentage of BDNF-IR DiI-labeled cell bodies in the NG (Fig. 5E), suggesting that BDNF is faithfully transported to the central targets. Due to a relatively long time course of DiI transport, it was not possible to examine BDNF distribution in specifically identified baroafferent

terminals at time points earlier than P30. However, we have found BDNF immunoreactivity in the solitary tract and the medial NTS as early as P1 (data not shown). Together, our data suggest that BDNF is likely to play a role at first-order baroreceptor synapses during both postnatal maturation and adult plasticity.

Bursting patterns of electrical stimulation known to induce plasticity in baroreceptor pathways are significantly more effective at releasing BDNF from nodose ganglion neurons than tonic patterns of the same average frequency

Expression of BDNF in baroafferent axons and terminal-like structures in the brainstem strongly suggests that BDNF is released at first-order baroreceptor synapses. In order to help establish physiological conditions under which BDNF is released from arterial baroreceptors, we examined the effects of stimulation patterns that mimic different levels of baroafferent activity *in vivo* on the release of native BDNF from dissociate cultures of NG neurons (Fig. 6A), which included the baroafferent population (Fig. 6B). We focused our study on patterns of baroreceptor activity known to evoke plastic changes at baroreceptor synapses, and asked whether the magnitude of BDNF release is regulated by these patterns. Seven stimulation protocols, each delivering the same overall number of pulses (20,000), were applied: 4 protocols of continuous stimulation, i.e. at 6 Hz, 12 Hz, 24 Hz and 48 Hz, were compared with 3 protocols of bursting patterns, i.e. 2 pulses at 36 Hz (mean frequency 12 Hz); 4 pulses at 72 Hz (mean frequency 24 Hz), and 8 pulses at 144 Hz (mean frequency 48 Hz), applied at 6 Hz, a frequency corresponding to a rat heart rate, as previously described by Liu *et al.* (2000). Following the initial 3-day culture period, sister NG cultures were stimulated using the protocols described above and schematically depicted in Figure 6C and D.

All stimulated cultures exhibited a significant increase in BDNF release compared to unstimulated controls. However, stimulation with patterns known to induce plastic changes in baroreceptor pathways was markedly more effective at releasing BDNF compared to tonic stimulation at the same average frequency (Fig. 6C, D). Moreover, the amount of released BDNF was regulated by inter-pulse frequency during phasic, but not tonic, stimulation (Fig. 6D). Together, the data indicate that the mechanisms regulating BDNF release from NG neurons discriminate among not only different frequencies but also patterns of stimulation, such that the release is facilitated selectively by high-frequency bursting patterns.

Patterned stimulation-evoked release of BDNF from nodose ganglion neurons requires both Land N-type calcium channels

Our earlier studies demonstrated that electrical stimulation-evoked BDNF release from NPG neurons is abolished by tetrodotoxin (TTX), an inhibitor of voltage-gated sodium channels (Balkowiec and Katz 2000). Also, we have previously shown that activity-dependent BDNF release from both sensory and hippocampal neurons requires calcium mobilization from intracellular stores (Balkowiec and Katz 2002; Buldyrev *et al.* 2006). The same studies revealed that the relative contribution of different calcium channels to activity-dependent BDNF release is cell type-specific (e.g. hippocampal vs. trigeminal ganglion cells; Balkowiec and Katz 2002; Buldyrev *et al.* 2006). Therefore, we next sought to determine which subtypes of voltage-activated calcium channels are involved in BDNF release from NG neurons.

Pretreatment of NG cultures with an L-type channel antagonist Nimodipine (2 μM) inhibited BDNF release by 25.8% during 1 h of 24-Hz continuous stimulation (Fig. 7). For the same stimulation paradigm, pretreatment with 1 μM ω-Conotoxin GVIA, an N-type calcium channel antagonist, inhibited BDNF release by 64 % (Fig. 7). Simultaneous application of both Nimodipine (2 μM) and ω-Conotoxin GVIA (1 μM) resulted in an abolition of BDNF release (Fig. 7). These data indicate that activity-dependent release of native BDNF from NG neurons

is controlled by calcium entry through both N- and L-type calcium channels, with a much stronger contribution by N-type calcium channels.

DISCUSSION

The current study provides the first direct evidence that BDNF is present in a large subset of arterial baroreceptor afferents, including their central axons in the brainstem solitary tract and terminal-like puncta in the *nucleus tractus solitarius* (NTS). BDNF is expressed in both A- and C-type baroreceptor afferents, during and after the period of postnatal maturational changes, indicating a potential for this neurotrophin to play a role in the plasticity of various baroreceptor reflexes activated under differing sensory inputs. BDNF release from nodose ganglion (NG) neurons is regulated by patterns that mimic baroreceptor activity *in vivo*, such that phasic baroreceptor firing patterns are markedly more effective at releasing BDNF than tonic patterns of the same average frequency. Furthermore, the release is largely dependent on activity of N-type voltage-gated calcium channels, known to be primarily expressed at synaptic terminals of NG neurons.

The arterial baroreceptor reflex, together with other cardiorespiratory reflexes, undergoes considerable maturational changes during the early postnatal period (Merrill *et al.* 1995; Segar 1997; Mazursky *et al.* 1998; Merrill *et al.* 1999; Ishii *et al.* 2001; Arsenault *et al.* 2003). Within the first two postnatal weeks in mice, the baroreflex gain increases nearly 4-fold to almost reach the adult value (Ishii *et al.* 2001). Several lines of evidence indicate that the first weeks of postnatal life bring significant changes to the NTS circuitry, which is the central target of cardiorespiratory afferents. These changes include morphological and electrophysiological maturation of NTS neurons and synaptic connections (Kalia 1992; Denavit-Saubie *et al.* 1994; Vincent and Tell 1997; Smith *et al.* 1998; Rao *et al.* 1999; Vincent and Tell 1999; Kawai and Senba 2000). Furthermore, changes in the NTS likely result in changes in reflex function as a whole. However, very little is known about molecular mechanisms that govern these changes.

The present study demonstrates that a large subset of baroreceptor neurons from both early postnatal and young adult rats expresses BDNF, the neurotrophin with a well-established role in developmental and adult plasticity of synaptic connections (Huang and Reichardt 2001), including sensory pathways (Malcangio and Lessmann 2003). Using young adult rats, we show that BDNF is present not only in baroreceptor cell bodies, but also their central projections. Unfortunately, our experimental approach using DiI tracing could not provide direct evidence for BDNF expression in the central projections of early postnatal baroreceptor neurons for technical reasons (i.e. inadequate time for the dye transport). However, the fact that BDNF is abundantly expressed in the early postnatal solitary tract as well as areas of the NTS known to receive baroafferent input, together with the evidence for the abundant expression of BDNF in early postnatal baroreceptor cell bodies, make the existence of BDNF in central axons and terminals of early postnatal baroafferents highly likely.

Previous studies, including a recent study from our laboratory, show that a significant fraction of BDNF within central axon terminals of sensory neurons is localized to dense-core vesicles (Michael *et al.* 1997; Buldyrev *et al.* 2006). These data, combined with the current findings, strongly suggest that BDNF is released at baroafferent synapses in the NTS by activity, indicating a potential role of BDNF in developmental and adult plasticity of baroreceptor pathways. This notion is supported by the fact that second-order sensory neurons in the NTS express the high-affinity receptor for BDNF, TrkB (Balkowiec *et al.* 2000). Moreover, very recent studies from other laboratories indicate that microinjections of the BDNF neutralizing antibody to the medial NTS lead to significant decreases in mean arterial blood pressure (Clark et al., 2008), suggesting a direct role of BDNF in baroafferent transmission in the NTS.

Baroreceptor afferents constitute a morphologically and functionally heterogenous population, with two major types of cells: thinly myelinated Aδ, associated with bursting patterns of baroreceptor activity, and unmyelinated C-type, distinguished by more tonic discharge patterns (Chapleau and Abboud 1989; Chapleau *et al.* 1989; Seagard *et al.* 1993). In an attempt to identify the subpopulation of baroreceptor neurons that expresses BDNF, we performed a thorough analysis of cell size distribution and colocalization studies with HCN1, a marker of A-type baroafferents (Doan *et al.*, 2004) and TRPV1, a marker of capsaicin-sensitive C-type baroafferents (Jin *et al.*, 2004). All lines of evidence indicate that BDNF is expressed by significant fractions (40–60%) of both A- and C-type baroreceptors. This raises the possibility that BDNF is involved only in select baroreflexes, or mobilized under certain physiological conditions. Since BDNF expression is regulated by activity, the BDNF-non-IR subpopulation could simply represent the “silent”, or less active, fraction of baroreceptor afferents. In support, BDNF protein is upregulated in DOCA-salt hypertensive rats compared to aged-matched controls (Jenkins *et al*, 2007). Similarly, the developmental decline in the number of BDNF-expressing baroafferents could be a result of changes in neuronal activity among various subpopulations of baroreceptor neurons. The cell size distribution analysis revealed that the proportion of BDNF-IR cells is greater in large, A-type, baroafferents, known to preferentially discharge with bursting patterns. This is consistent with another observation from this study that the magnitude of BDNF release from NG neurons is significantly higher in response to bursting, compared to tonic patterns of activation.

It is not possible at the present time to measure BDNF released exclusively from the baroreceptor population of NG neurons. For that reason, we chose to examine the effects of baroreceptor patterns of stimulation on BDNF release from dispersed NG neurons. Although NG cultures contain, in addition to baroafferents, other functionally distinct populations of sensory neurons, baroreceptor afferents retain BDNF expression *in vitro* (Fig. 3B) and, therefore, are very likely to contribute to the detected BDNF release. Moreover, previous studies strongly suggest that baroreceptor afferent pathways do not differ from other NG afferent pathways with respect to stimulus-response characteristics at first-order synapses in the NTS (Mifflin 1997;Bailey *et al.* 2006).

Our results show that the stimulus-evoked BDNF release from NG neurons is largely dependent on N-type calcium channels. In turn, N-type channels are present predominantly at synaptic terminals of NG neurons, as previously demonstrated (Mendelowitz *et al.* 1995). Although our *in vitro* model of activity-dependent BDNF release does not allow for a direct determination of the subcellular sites of the release, these data are consistent with the hypothesis that BDNF release occurs at central terminals of baroreceptor afferents.

Our data indicate that the mechanisms regulating BDNF release from NG neurons discriminate among not only different frequencies but also patterns of stimulation, such that the release is enhanced during high-frequency bursts delivered at the heart rate frequency. These data are consistent with previous studies of BDNF release from other neuronal populations, including dorsal root ganglion (Lever et al., 2001) and hippocampal (Balkowiec and Katz, 2002) neurons. It is well established that many baroreceptor afferents provide a bursting input to the NTS that is synchronous with the systolic phase of the cardiac cycle (Chapleau and Abboud 1989; Chapleau *et al.* 1989; Seagard *et al.* 1993). Moreover, the pattern of baroreceptor activity determines the magnitude of the reflex response independently of the mean frequency of baroreceptor discharges, with pulsatile activation leading to central facilitation of the reflex (Chapleau and Abboud 1987, 1989). Therefore, there is a possibility that BDNF, released in large quantities from a subpopulation of baroreceptor afferents during their pulsatile activation, contributes to the baroreflex facilitation. In support of this possibility, we found that BDNF is expressed in a significant fraction of larger, A-type baroafferents, which are characterized by bursting patterns of activity. We also determined that BDNF is expressed in baroreceptor

afferents beyond the period of postnatal maturational changes. Consequently, BDNF is likely to play a role in adult plasticity of selected baroreflexes.

In addition to baroreflex facilitation, phenomena representing other forms of synaptic plasticity at baroreceptor synapses have been described. For example, the magnitude of postsynaptic responses in NTS neurons is regulated by the frequency of the presynaptic input. Specifically, increasing the frequency of baroreceptor input leads to depression of postsynaptic responses in NTS neurons (Scheuer *et al.* 1996; Liu *et al.* 1998; Chen *et al.* 1999; Liu *et al.* 2000; Doyle and Andresen 2001), the phenomenon known as 'frequency-dependent depression' (FDD), which may influence the function of the baroreceptor reflex (Liu *et al.* 2000). Several mechanisms have been implicated to contribute to FDD, including alterations in presynaptic mechanisms (Schild *et al.* 1995; Chen *et al.* 1999), desensitization of non-NMDA receptors (Schild *et al.* 1995; Zhou *et al.* 1997), an adenylate cyclase-mediated regulatory mechanism (Schild *et al.* 1995), activation of presynaptic metabotropic glutamate receptors (Liu *et al.* 1998), activation of mu-opiate receptors (Hamra *et al.* 1999), and frequency-dependent depression of endocytosis (Pamidimukkala and Hay 2001). In the present study, the patterns known to evoke very pronounced FDD were most effective at releasing BDNF. Previously, we demonstrated that exogenous BDNF acutely inhibits AMPA currents in second-order sensory neurons in the NTS (Balkowiec *et al.* 2000). These data, in conjunction with the evidence that glutamate receptors mediate baroreceptor afferent transmission in the NTS (Guyenet *et al.* 1987; Andresen and Yang 1990; Drewe *et al.* 1990; Gordon and Leone 1991; Lawrence and Jarrott 1994; Zhang and Mifflin 1995; Aylwin *et al.* 1997; Andresen *et al.* 2001; Gordon and Sved 2002; Schreihofer and Guyenet 2002; Guyenet 2006), indicate that BDNF may be involved in the mechanisms of FDD.

In conclusion, the present study identifies BDNF as a likely mediator of activity-dependent modifications at first-order synapses in arterial baroreceptor pathways, including postnatal maturation of the baroreceptor reflex. These data may be relevant to understanding the pathomechanisms of developmental disorders of the cardio-respiratory system, such as Sudden Infant Death Syndrome (SIDS).

Acknowledgements

A.B. would like to thank Dr. David M. Katz of Case Western Reserve University, Cleveland, OH, for his invaluable support at initial stages of the project development. The authors express their gratitude to Dr. Michael Danilchik for help with the confocal microscopy portion of this study. This work was supported by grants from the American Heart Association (0230095N) and the National Heart, Lung, and Blood Institute of the National Institutes of Health (HL076113) to A.B.

Abbreviations

ADN
: aortic depressor nerve

AMPA
: alpha-amino-3-hydoxy-5-methylisoxazole-4-propionate

BDNF
: brain-derived neurotrophic factor

CM-DiI
: Chloromethylbenzamido-1,1′-dioctadecyl-3,3,3′,3′-tetramethylindocarbocyanine perchlorate

FDD

frequency-dependent depression

HCN1
hyperpolarization-activated cyclic nucleotide-gated ion channel protein 1

IR
immunoreactive or immunoreactivity

NG
nodose ganglion

NPG
nodose-petrosal ganglion complex

NTS
nucleus tractus solitarius

P
postnatal day

PBS
phosphate-buffered saline

TRPV1
transient receptor potential vanilloid type 1

References

Andresen MC, Doyle MW, Jin YH, Bailey TW. Cellular mechanisms of baroreceptor integration at the nucleus tractus solitarius. Ann N Y Acad Sci 2001;940:132–141. [PubMed: 11458672]

Andresen MC, Kunze DL. Nucleus tractus solitarius--gateway to neural circulatory control. Annu Rev Physiol 1994;56:93–116. [PubMed: 7912060]

Andresen MC, Yang M. Arterial baroreceptor resetting: contributions of chronic and acute processes. Clin Exp Pharmacol Physiol Suppl 1989;15:19–30. [PubMed: 2805444]

Andresen MC, Yang MY. Non-NMDA receptors mediate sensory afferent synaptic transmission in medial nucleus tractus solitarius. Am J Physiol 1990;259:H1307–1311. [PubMed: 1977326]

Apfel SC, Wright DE, Wiideman AM, Dormia C, Snider WD, Kessler JA. Nerve growth factor regulates the expression of brain-derived neurotrophic factor mRNA in the peripheral nervous system. Mol Cell Neurosci 1996;7:134–142. [PubMed: 8731481]

Arsenault J, Moreau-Bussiere F, Reix P, Niyonsenga T, Praud JP. Postnatal maturation of vagal respiratory reflexes in preterm and full-term lambs. J Appl Physiol 2003;94:1978–1986. [PubMed: 12547837]

Aylwin ML, Horowitz JM, Bonham AC. NMDA receptors contribute to primary visceral afferent transmission in the nucleus of the solitary tract. J Neurophysiol 1997;77:2539–2548. [PubMed: 9163375]

Bailey TW, Hermes SM, Andresen MC, Aicher SA. Cranial visceral afferent pathways through the nucleus of the solitary tract to caudal ventrolateral medulla or paraventricular hypothalamus: target-specific synaptic reliability and convergence patterns. J Neurosci 2006;26:11893–11902. [PubMed: 17108163]

Balkowiec A, Katz DM. Activity-dependent release of endogenous brain-derived neurotrophic factor from primary sensory neurons detected by ELISA in situ. J Neurosci 2000;20:7417–7423. [PubMed: 11007900]

Balkowiec A, Katz DM. Cellular mechanisms regulating activity-dependent release of native brain-derived neurotrophic factor from hippocampal neurons. J Neurosci 2002;22:10399–10407. [PubMed: 12451139]

Balkowiec A, Kunze DL, Katz DM. Brain-derived neurotrophic factor acutely inhibits AMPA-mediated currents in developing sensory relay neurons. J Neurosci 2000;20:1904–1911. [PubMed: 10684891]

Bennett HL, Gustafsson JA, Keast JR. Estrogen receptor expression in lumbosacral dorsal root ganglion cells innervating the female rat urinary bladder. Auton Neurosci Basic Clin 2003;105:90–100.

Brady R, Zaidi SIA, Mayer C, Katz DM. BDNF is a target-derived survival factor for arterial baroreceptor and chemoafferent primary sensory neurons. J Neurosci 1999;19:2131–2142. [PubMed: 10066266]

Brooks VL, Sved AF. Pressure to change? Re-evaluating the role of baroreceptors in the long-term control of arterial pressure. Am J Physiol 2005;288:R815–818.

Buldyrev I, Tanner NM, Hsieh HY, Dodd EG, Nguyen LT, Balkowiec A. Calcitonin gene-related peptide enhances release of native brain-derived neurotrophic factor from trigeminal ganglion neurons. J Neurochem 2006;99:1338–1350. [PubMed: 17064360]

Chapleau MW, Abboud FM. Contrasting effects of static and pulsatile pressure on carotid baroreceptor activity in dogs. Circ Res 1987;61:648–658. [PubMed: 3664974]

Chapleau MW, Abboud FM. Determinants of sensitization of carotid baroreceptors by pulsatile pressure in dogs. Circ Res 1989;65:566–577. [PubMed: 2766484]

Chapleau MW, Hajduczok G, Abboud FM. Pulsatile activation of baroreceptors causes central facilitation of baroreflex. Am J Physiol 1989;256:H1735–1741. [PubMed: 2735443]

Chen CY, Horowitz JM, Bonham AC. A presynaptic mechanism contributes to depression of autonomic signal transmission in NTS. Am J Physiol 1999;277:H1350–1360. [PubMed: 10516169]

Cheng Z, Powley TL, Schwaber JS, Doyle FJ 3rd. A laser confocal microscopic study of vagal afferent innervation of rat aortic arch: chemoreceptors as well as baroreceptors. J Auton Nerv Syst 1997;67:1–14. [PubMed: 9470139]

Clark CG, Kline DD, Kunze DL, Katz DM, Hasser EM. The role of brain derived neurotrophic factor on autonomic and cardiovascular function. Soc Neurosci Abstr 2008:676.7.

Denavit-Saubie M, Kalia M, Pierrefiche O, Schweitzer P, Foutz AS, Champagnat J. Maturation of brain stem neurons involved in respiratory rhythmogenesis: biochemical, bioelectrical and morphological properties. Biol Neonate 1994;65:171–175. [PubMed: 8038279]

Doan TN, Stephans K, Ramirez AN, Glazebrook PA, Andresen MC, Kunze DL. Differential distribution and function of hyperpolarization-activated channels in sensory neurons and mechanosensitive fibers. J Neurosci 2004;24:3335–3343. [PubMed: 15056713]

Doyle MW, Andresen MC. Reliability of monosynaptic sensory transmission in brain stem neurons in vitro. J Neurophysiol 2001;85:2213–2223. [PubMed: 11353036]

Drewe JA, Miles R, Kunze DL. Excitatory amino acid receptors of guinea pig medial nucleus tractus solitarius neurons. Am J Physiol 1990;259:H1389–1395. [PubMed: 1978575]

Erickson JT, Conover JC, Borday V, Champagnat J, Barbacid M, Yancopoulos G, Katz DM. Mice lacking brain-derived neurotrophic factor exhibit visceral sensory neuron losses distinct from mice lacking NT4 and display a severe developmental deficit in control of breathing. J Neurosci 1996;16:5361–5371. [PubMed: 8757249]

Gordon FJ, Leone C. Non-NMDA receptors in the nucleus of the tractus solitarius play the predominant role in mediating aortic baroreceptor reflexes. Brain Res 1991;568:319–322. [PubMed: 1687671]

Gordon FJ, Sved AF. Neurotransmitters in central cardiovascular regulation: glutamate and GABA. Clin Exp Pharmacol Physiol 2002;29:522–524. [PubMed: 12010202]

Guyenet PG. The sympathetic control of blood pressure. Nature Rev Neurosci 2006;7:335–346. [PubMed: 16760914]

Guyenet PG, Filtz TM, Donaldson SR. Role of excitatory amino acids in rat vagal and sympathetic baroreflexes. Brain Res 1987;407:272–284. [PubMed: 3567646]

Hamra M, McNeil RS, Runciman M, Kunze DL. Opioid modulation of calcium current in cultured sensory neurons: mu-modulation of baroreceptor input. Am J Physiol 1999;277:H705–713. [PubMed: 10444497]

Heesch CM, Abboud FM, Thames MD. Acute resetting of carotid sinus baroreceptors. II. Possible involvement of electrogenic Na+ pump. Am J Physiol 1984a;247:H833–839. [PubMed: 6093597]

Heesch CM, Thames MD, Abboud FM. Acute resetting of carotid sinus baroreceptors. I. Dissociation between discharge and wall changes. Am J Physiol 1984b;247:H824–832. [PubMed: 6496763]

Huang EJ, Reichardt LF. Neurotrophins: roles in neuronal development and function. Annu Rev Neurosci 2001;24:677–736. [PubMed: 11520916]

Ichikawa H, Terayama R, Yamaai T, Yan Z, Sugimoto T. Brain-derived neurotrophic factor-immunoreactive neurons in the rat vagal and glossopharyngeal sensory ganglia; co-expression with other neurochemical substances. Brain Res 2007;1155:93–99. [PubMed: 17512913]

Ishii T, Kuwaki T, Masuda Y, Fukuda Y. Postnatal development of blood pressure and baroreflex in mice. Auton Neurosci 2001;94:34–41. [PubMed: 11775705]

Jenkins VK, Pricher M, O'Donaughy T, Hsieh H-Y, Brooks VL, Balkowiec A. Activity-dependent regulation of BDNF expression in nodose ganglia of DOCA-salt hypertensive rats. Soc Neurosci Abstr 2007:139.11.

Jin YH, Bailey TW, Li BY, Schild JH, Andresen MC. Purinergic and vanilloid receptor activation releases glutamate from separate cranial afferent terminals in nucleus tractus solitarius. J Neurosci 2004;24:4709–4717. [PubMed: 15152030]

Kalia M. Early ontogeny of the vagus nerve: an analysis of the medulla oblongata and cervical spinal cord of the postnatal rat. Neurochem Int 1992;20:119–128. [PubMed: 1284677]

Kawai Y, Senba E. Postnatal differentiation of local networks in the nucleus of the tractus solitarius. Neuroscience 2000;100:109–114. [PubMed: 10996462]

Kunze DL. Rapid resetting of the carotid baroreceptor reflex in the cat. Am J Physiol 1981;241:H802–806. [PubMed: 7325247]

Kunze DL. Acute resetting of baroreceptor reflex in rabbits: a central component. Am J Physiol 1986;250:H866–870. [PubMed: 3706559]

Lawrence AJ, Jarrott B. L-glutamate as a neurotransmitter at baroreceptor afferents: evidence from in vivo microdialysis. Neuroscience 1994;58:585–591. [PubMed: 7909588]

Lever IJ, Bradbury EJ, Cunningham JR, Adelson DW, Jones MG, McMahon SB, Marvizon JC, Malcangio M. Brain-derived neurotrophic factor is released in the dorsal horn by distinctive patterns of afferent fiber stimulation. J Neurosci 2001;21:4469–4477. [PubMed: 11404434]

Liu Z, Chen CY, Bonham AC. Frequency limits on aortic baroreceptor input to nucleus tractus solitarii. Am J Physiol 2000;278:H577–585.

Liu Z, Chen CY, Bonham AC. Metabotropic glutamate receptors depress vagal and aortic baroreceptor signal transmission in the NTS. Am J Physiol 1998;275:H1682–1694. [PubMed: 9815076]

Malcangio M, Lessmann V. A common thread for pain and memory synapses? Brain-derived neurotrophic factor and trkB receptors. Trends Pharmacol Sci 2003;24:116–121. [PubMed: 12628355]

Mazursky JE, Birkett CL, Bedell KA, Ben-Haim SA, Segar JL. Development of baroreflex influences on heart rate variability in preterm infants. Early Hum Dev 1998;53:37–52. [PubMed: 10193925]

Mendelowitz D, Reynolds PJ, Andresen MC. Heterogeneous functional expression of calcium channels at sensory and synaptic regions in nodose neurons. J Neurophysiol 1995;73:872–875. [PubMed: 7760142]

Merrill DC, McWeeny OJ, Segar JL, Robillard JE. Impairment of cardiopulmonary baroreflexes during the newborn period. Am J Physiol 1995;268:H1343–1351. [PubMed: 7900887]

Merrill DC, Segar JL, McWeeny OJ, Robillard JE. Sympathetic responses to cardiopulmonary vagal afferent stimulation during development. Am J Physiol 1999;277:H1311–1316. [PubMed: 10516165]

Michael GJ, Averill S, Nitkunan A, Rattray M, Bennett DL, Yan Q, Priestley JV. Nerve growth factor treatment increases brain-derived neurotrophic factor selectively in TrkA-expressing dorsal root ganglion cells and in their central terminations within the spinal cord. J Neurosci 1997;17:8476–8490. [PubMed: 9334420]

Mifflin SW. Short-term potentiation of carotid sinus nerve inputs to neurons in the nucleus of the solitary tract. Respir Physiol 1997;110:229–236. [PubMed: 9407615]

Pamidimukkala J, Hay M. Frequency dependence of endocytosis in aortic baroreceptor neurons and role of group III mGluRs. Am J Physiol 2001;281:H387–395.

Poo MM. Neurotrophins as synaptic modulators. Nature Rev Neurosci 2001;2:24–32. [PubMed: 11253356]

Rao H, Pio J, Kessler JP. Postnatal development of synaptophysin immunoreactivity in the rat nucleus tractus solitarii and caudal ventrolateral medulla. Brain Res Dev Brain Res 1999;112:281–285.

Reynolds PJ, Fan W, Andresen MC. Capsaicin-resistant arterial baroreceptors. J Negat Results Biomed 2006;5:6. [PubMed: 16709252]

Schecterson LC, Bothwell M. Novel roles for neurotrophins are suggested by BDNF and NT-3 mRNA expression in developing neurons. Neuron 1992;9:449–463. [PubMed: 1345671]

Scheuer DA, Zhang J, Toney GM, Mifflin SW. Temporal processing of aortic nerve evoked activity in the nucleus of the solitary tract. J Neurophysiol 1996;76:3750–3757. [PubMed: 8985873]

Schild JH, Clark JW, Canavier CC, Kunze DL, Andresen MC. Afferent synaptic drive of rat medial nucleus tractus solitarius neurons: dynamic simulation of graded vesicular mobilization, release, and non-NMDA receptor kinetics. J Neurophysiol 1995;74:1529–1548. [PubMed: 8989391]

Schreihofer AM, Guyenet PG. The baroreflex and beyond: control of sympathetic vasomotor tone by GABAergic neurons in the ventrolateral medulla. Clin Exp Pharmacol Physiol 2002;29:514–521. [PubMed: 12010201]

Seagard JL, Hopp FA, Drummond HA, Van Wynsberghe DM. Selective contribution of two types of carotid sinus baroreceptors to the control of blood pressure. Circ Res 1993;72:1011–1022. [PubMed: 8477517]

Segar JL. Ontogeny of the arterial and cardiopulmonary baroreflex during fetal and postnatal life. Am J Physiol 1997;273:R457–471. [PubMed: 9277527]

Smith BN, Dou P, Barber WD, Dudek FE. Vagally evoked synaptic currents in the immature rat nucleus tractus solitarii in an intact *in vitro* preparation. J Physiol (Lond) 1998;512:149–162. [PubMed: 9729625]

Vincent A, Tell F. Postnatal changes in electrophysiological properties of rat nucleus tractus solitarii neurons. Eur J Neurosci 1997;9:1612–1624. [PubMed: 9283816]

Vincent A, Tell F. Postnatal development of rat nucleus tractus solitarius neurons: morphological and electrophysiological evidence. Neuroscience 1999;93:293–305. [PubMed: 10430493]

Wetmore C, Olson L. Neuronal and nonneuronal expression of neurotrophins and their receptors in sensory and sympathetic ganglia suggest new intercellular trophic interactions. J Comp Neurol 1995;353:143–159. [PubMed: 7714245]

Xie PL, McDowell TS, Chapleau MW, Hajduczok G, Abboud FM. Rapid baroreceptor resetting in chronic hypertension. Implications for normalization of arterial pressure. Hypertension 1991;17:72–79. [PubMed: 1986984]

Zhang W, Mifflin SW. Excitatory amino-acid receptors contribute to carotid sinus and vagus nerve evoked excitation of neurons in the nucleus of the tractus solitarius. J Auton Nerv Syst 1995;55:50–56. [PubMed: 8690851]

Zhou XF, Chie ET, Rush RA. Distribution of brain-derived neurotrophic factor in cranial and spinal ganglia. Exp Neurol 1998;149:237–242. [PubMed: 9454633]

Zhou XF, Rush RA. Endogenous brain-derived neurotrophic factor is anterogradely transported in primary sensory neurons. Neuroscience 1996;74:945–953. [PubMed: 8895863]

Zhou Z, Champagnat J, Poon CS. Phasic and long-term depression in brainstem nucleus tractus solitarius neurons: differing roles of AMPA receptor desensitization. J Neurosci 1997;17:5349–5356. [PubMed: 9204919]

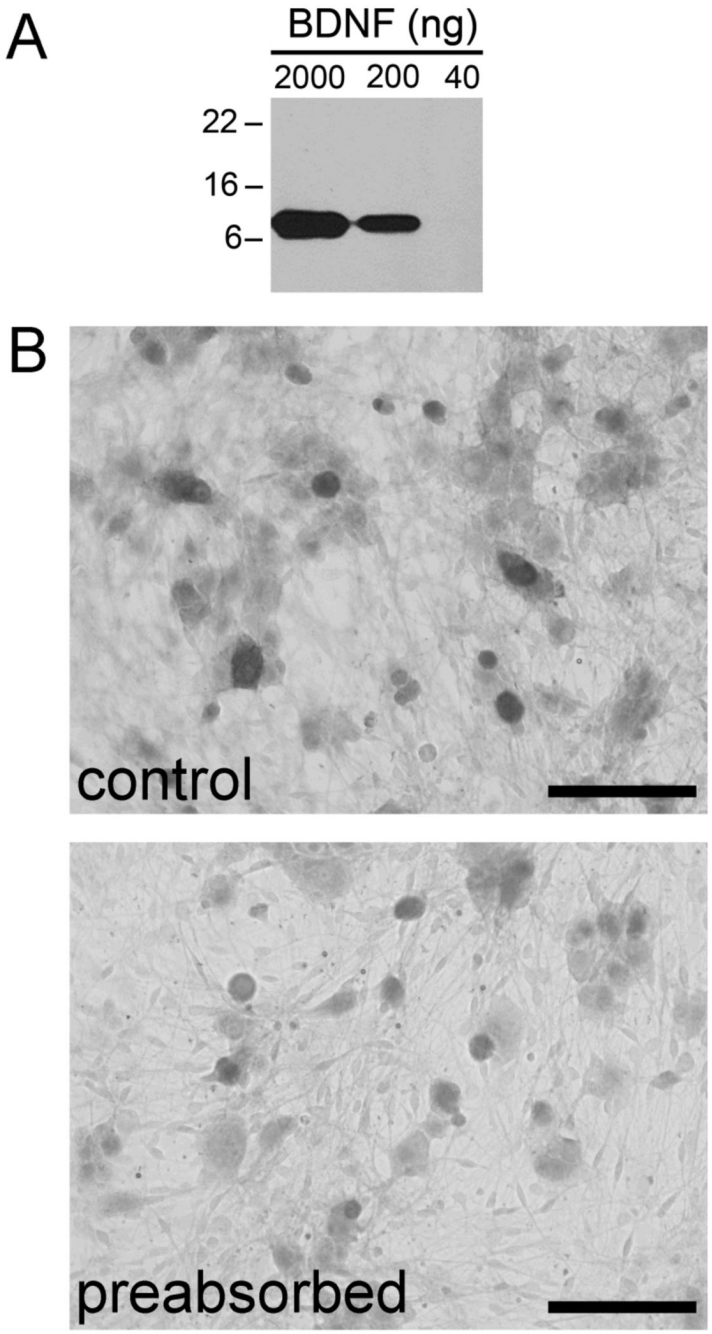

Figure 1. Chicken anti-BDNF polyclonal antibody preabsorbed with BDNF protein is ineffective in detecting endogenous BDNF in NG neurons

A, The results of Western blotting performed using 2000 ng, 200 ng, and 40 ng samples of recombinant human BDNF protein and the chicken anti-BDNF antibody. BDNF was reduced to approximately 13-kDa monomers by boiling in loading buffer containing 4.6% SDS and 5% β-mercaptoethanol. *B*, A dissociate 3-day culture of newborn rat NG neurons, immunostained with the BDNF antibody in control conditions (control) and following preabsorption with BDNF bound to magnetic beads. Scale bar, 100 μm.

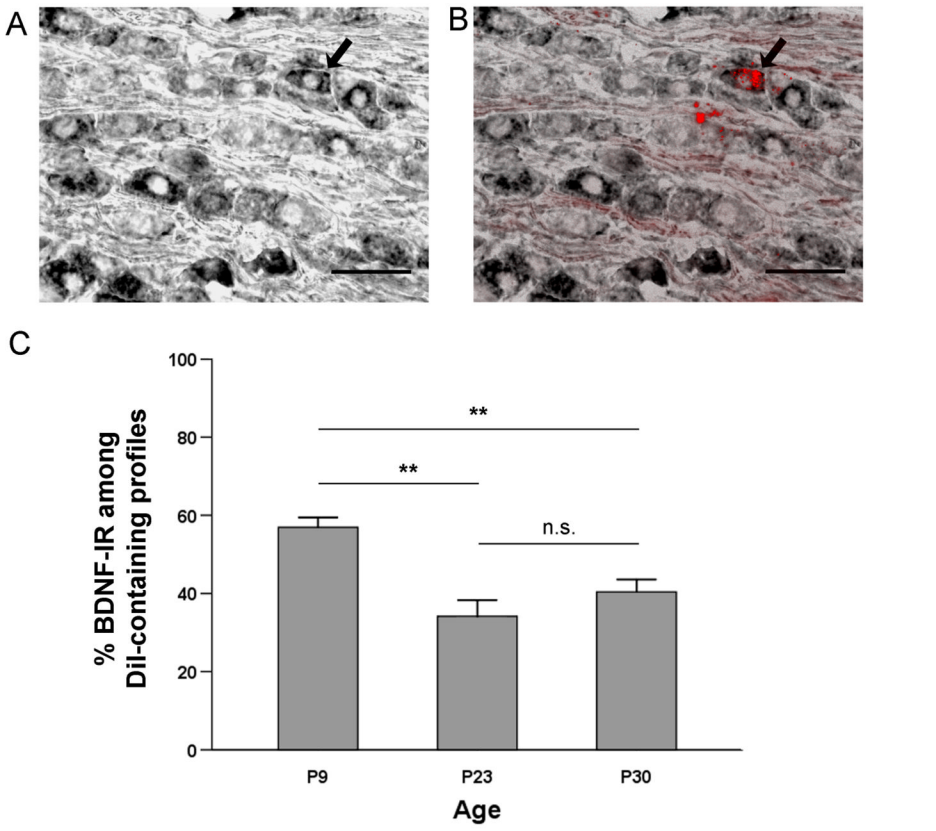

Figure 2. Cell bodies of putative baroafferent neurons in the nodose ganglion show abundant BDNF immunoreactivity from postnatal development into adulthood

A, A section through the right nodose ganglion immunostained for BDNF (ABC method) from a postnatal day (P) 23 rat in which CM-DiI was placed on the right aortic depressor nerve at P2. *B*, DiI fluorescence overlay of the same section. Arrows indicate a BDNF-positive neuron which is also labeled with DiI, suggesting its baroreceptor origin. Scale bar, 50 μm. *C*, Mean percentage of BDNF-IR cells within the DiI-labeled NG somata (putative baroafferents) in P9 (n=6), P23 (n=3), and P30 rats (n=5); ** $p<0.01$, n.s. = not significant.

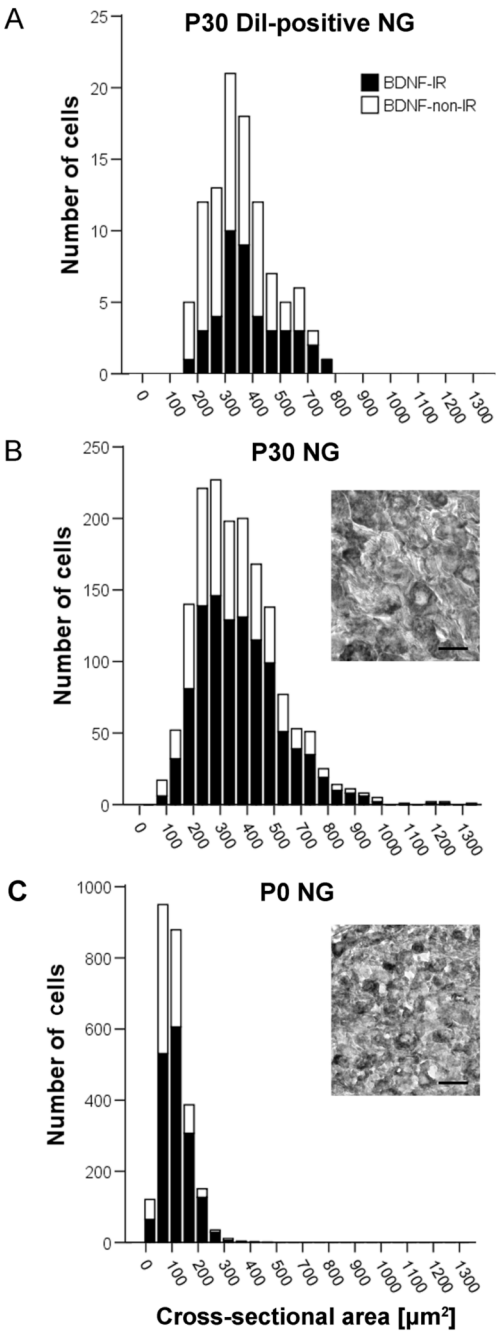

Figure 3. BDNF IR is present in baroafferent neurons of all sizes

A, Frequency distribution of the cross-sectional areas of DiI-positive somata from three P30 rats sampled from every other section through the NG. Frequency distribution of the cross-sectional areas of P30 (*B*) and P0 (*C*) NG somata taken from ganglion sections spaced approximately 110 µm apart. The data represent the combined number of cells obtained from three ganglia. *Insets*, example images of a section of P30 (*B*) and P0 (*C*) NG immunostained for BDNF (ABC method). Scale bar, 25 µm. Black bars, BDNF-IR; white bars, BDNF-non-IR. Sum of black bar and white bar represents the entire population sampled.

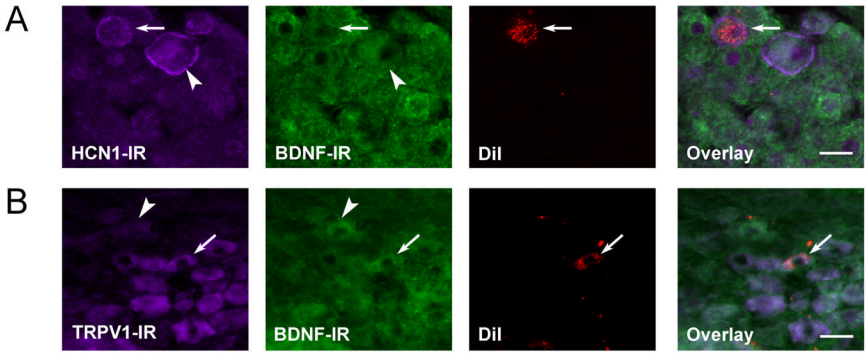

Figure 4. BDNF-IR is present in two distinct populations of NG neurons: lightly myelinated A-fibers (HCN1-IR) and unmyelinated C-fibers (TRPV1-IR)

Double immunofluorescence of HCN1 IR (*A*) or TRPV1 IR (*B*) and BDNF IR in a P30 rat, in which the neuronal tracer DiI was placed on the ADN at P2. In *A*, The arrow indicates a putative baroafferent neuron containing HCN1 IR, but negative for BDNF IR. The arrowhead points to an NG cell that is HCN1 immunoreactive, as well as BDNF immunoreactive. HCN1 IR is characterized by a bright, cell membrane staining in medium to larger neurons. In *B*, the arrow points to a putative baroafferent neuron positive for TRPV1 and BDNF. The arrowhead indicates an NG cell that is TRPV1-non-IR, but positive for BDNF.

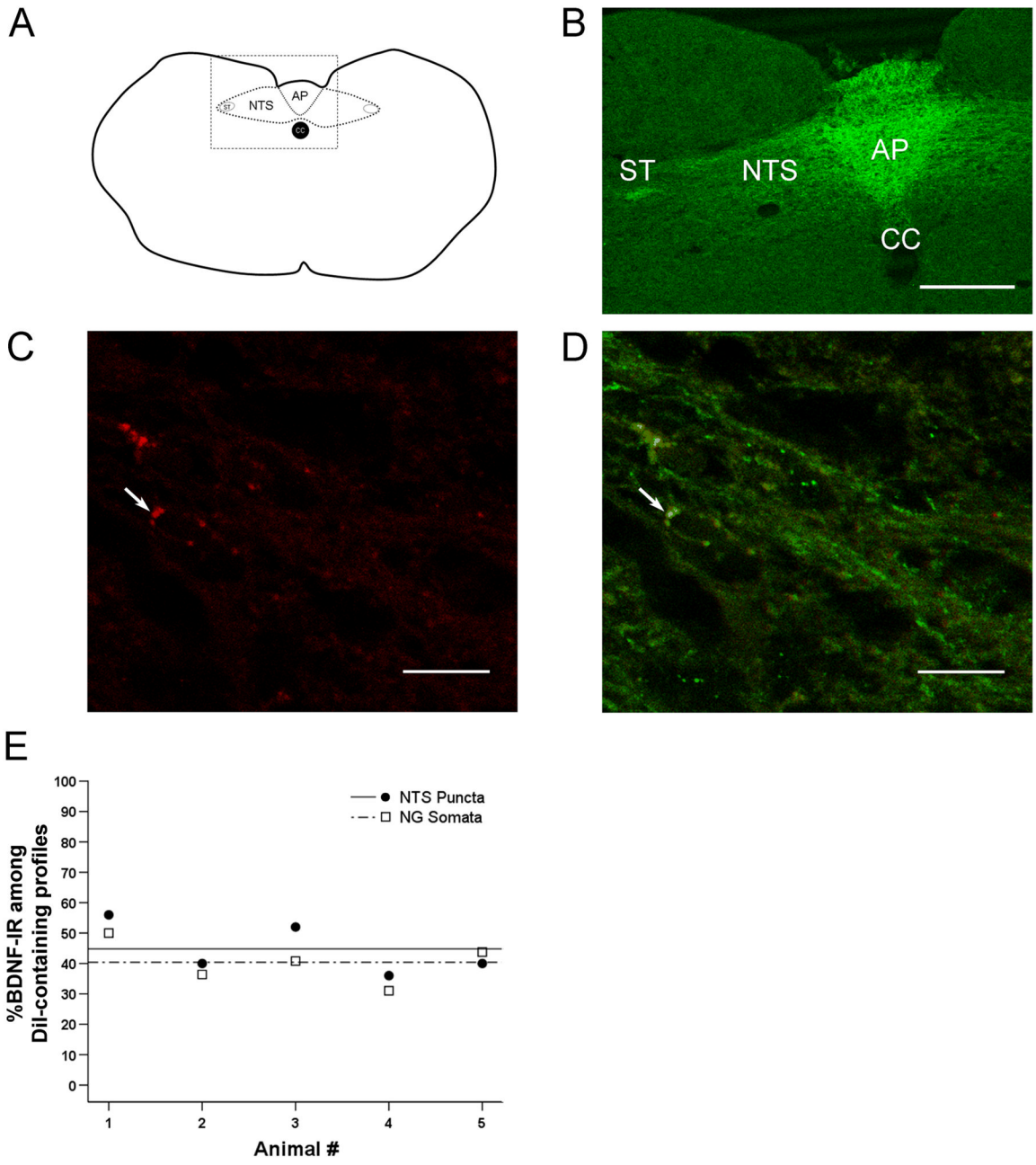

Figure 5. BDNF immunoreactivity (-IR) is present in the terminal field of nodose ganglion visceral sensory neurons in the *nucleus tractus solitarius* (NTS), including putative baroafferents

A, Schematic of a cross-section through the caudal brainstem. AP, area postrema; NTS, *nucleus tractus solitarius*; ST, solitary tract; CC, central canal. Box represents the field of view seen in *B*. *B*, Laser scanning confocal image through the caudal brainstem of a postnatal day (P) 30 rat showing strong BDNF IR in the NTS, which contains terminations of nodose ganglion (NG) neurons, including baroreceptor afferents. BDNF IR is also present in the ST, suggesting that BDNF is transported in NG afferents to their terminals in the NTS. Scale bar, 250 μm. *C*, High magnification laser scanning confocal image showing terminal-like puncta of DiI-positive, putative baroafferent neurons (red). *D*. Overlay of DiI (red) and BDNF IR (green). Arrows indicate a punctum in which DiI and BDNF IR colocalize (yellow). Scale bar, 10 μm. *E*, The

percentage of BDNF-IR somata (open squares) and medial NTS puncta (filled circles) shown for individual P30 animals analyzed. Percentages of BDNF IR calculated for NG somata closely match the percentages obtained for NTS puncta, further supporting the hypothesis that BDNF expressed in the cell bodies of baroreceptor neurons is faithfully transported to afferent terminals in the brainstem. The mean percentage of BDNF-IR profiles within the putative baroafferent population does not significantly differ between NG somata (dashed line) and NTS puncta (solid line) across individual animals, $p=0.41$.

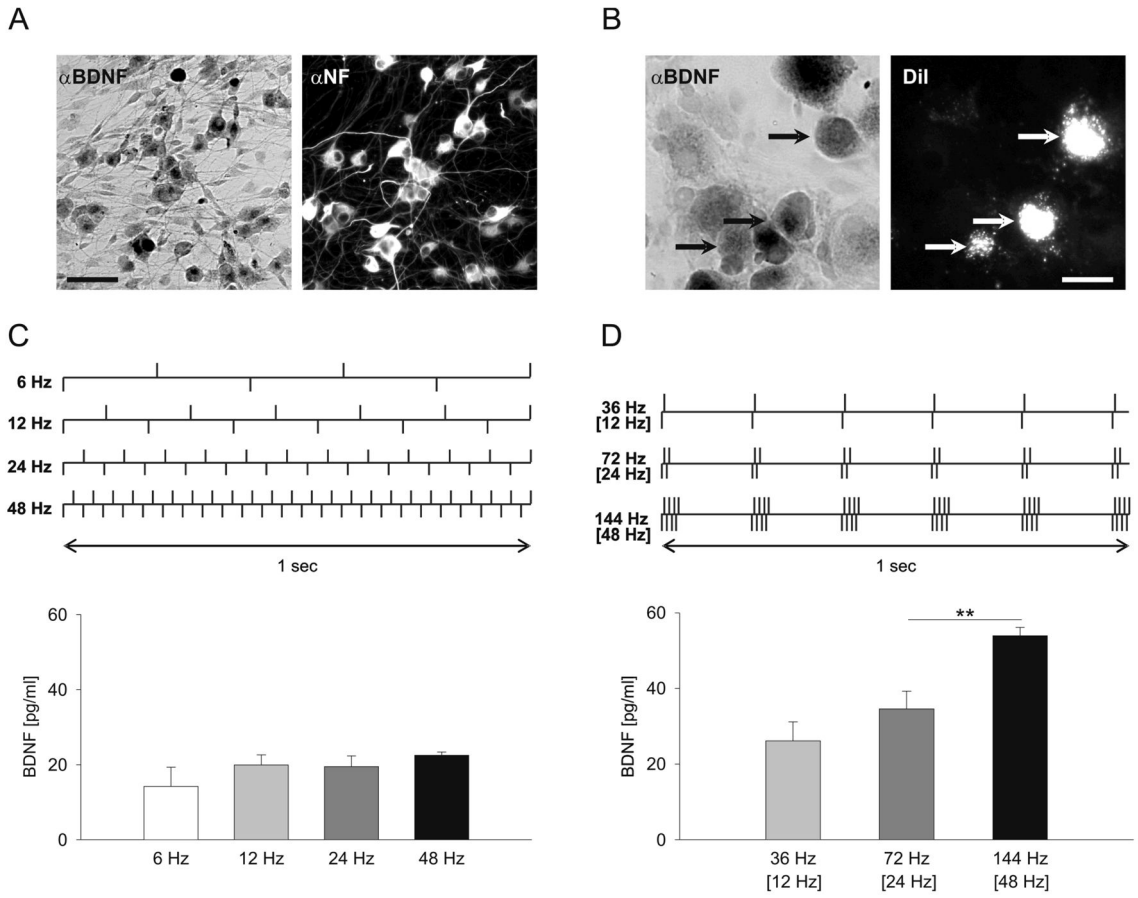

Figure 6. Endogenous BDNF is released from newborn nodose ganglion (NG) neurons *in vitro* by physiological patterns of baroreceptor activity

A, A representative example of a dissociate 3-day culture of newborn rat NGs, double-immunostained for BDNF (αBDNF) and Neurofilament (αNF). Scale bar, 60 μm. *B*, BDNF-immunoreactivity (αBDNF) in a dissociate 1-day culture of NGs from postnatal day (P) 9 rats, in which both aortic depressor nerves were pre-labeled with the fluorescent tracer CM-DiI (DiI) at P2. Arrows indicate three BDNF-positive neurons (αBDNF, black arrows) that are also DiI-labeled (DiI, white arrows), indicating their putative baroreceptor origin. Scale bar, 15 μm. *C*, *D*, *top*, Schematic representation of stimulation patterns delivered to sister 3-day cultures of newborn NG neurons. *C*, *D*, *bottom*, Mean above control levels of BDNF released during electrical field stimulation delivered continuously at 6 Hz (55.6 min), 12 Hz (27.8 min), 24 Hz (13.9 min) or 48 Hz (6.95 min; *C*), or as bursts of 2, 4 or 8 pulses, with intraburst/[average] frequencies of 36 Hz/[12 Hz], 72 Hz/[24 Hz] and 144 Hz/[48 Hz], respectively (*D*). The total number of delivered pulses was the same for all stimulation protocols. A total of three independent experiments, each containing four cultures per stimulation pattern, were performed; ** $p<0.01$.

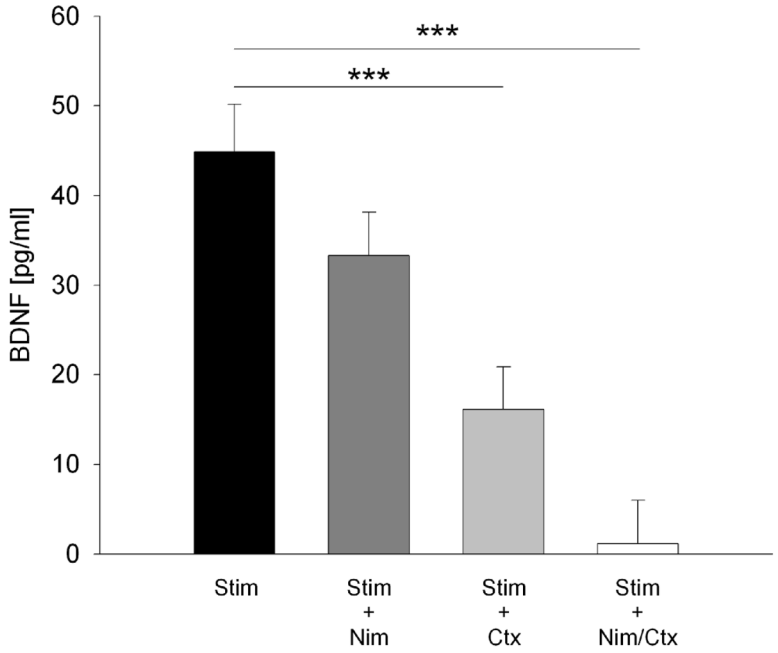

Figure 7. Release of endogenous BDNF evoked by patterned electrical stimulation of newborn NG neurons requires calcium influx through L- and N-type channels

Mean above vehicle-control levels of BDNF released in sister cultures of newborn NG neurons during one hour of continuous electrical field stimulation at 24 Hz in the absence (Stim; n=18) or presence of voltage-activated calcium channel antagonists: 2 μM Nimodipine, an L-type channel antagonist (Stim + Nim; n=12), 1 μM ω-Conotoxin GVIA, an N-type channel antagonist (Stim + Ctx; n=13), or both applied simultaneously (Stim + Nim/Ctx; n=7); *** $p<0.001$.

TABLE 1

Quantification of BDNF-IR DiI-labeled cell bodies of NG neurons (putative baroafferents) within HCN1- and TRPV1-IR and non-IR subpopulations

Somata that were analyzed for HCN1 IR or TRPV1 IR were further assessed for BDNF IR. Data are derived from two nodose ganglia (NG) of two P30 rats that were pre-labeled with DiI applied to the aortic depressor nerve at P2. Double immunofluorescent staining was performed on alternate sections of the same NG for HCN1-IR and BDNF-IR or TRPV1-IR and BDNF-IR, respectively. All DiI-positive somata containing a nucleus were assessed.

	DiI-labeled Cell Bodies (Putative Baroafferents) %	BDNF-IR DiI-labeled Cell Bodies (Putative Baroafferents) %
HCN1-IR	21.36 ± 0.85	43.75 ± 6.25
HCN1-non-IR	78.64 ± 0.85	48.48 ± 0.09
TRPV1-IR	51.47 ± 6.02	58.26 ± 1.74
TRPV1-non-IR	48.53 ± 6.02	31.37 ± 1.96